Supplementary Information

Two-gap topological superconductor LaB_2 with high $T_C = 30$ K

Chin-Hsuan Chen,* Ye-Shun Lan,* and Angus Huang
Department of Physics, National Tsing Hua University, Hsinchu 30013, Taiwan

Horng-Tay Jeng†
Department of Physics, National Tsing Hua University, Hsinchu 30013, Taiwan
Institute of Physics, Academia Sinica, Taipei 11529, Taiwan and
Physics Division, National Center for Theoretical Sciences, Hsinchu 30013, Taiwan
(Dated: October 19, 2023)

I. EPC AND SUPERCONDUCTING GAP DISTRIBUTIONS OVER THE FS OF LAB_2.

The calculated EPC and superconducting gap distributions on FS are depicted in Fig. S1. Fig. S1(a) shows EPC strength distribution over the FS. The red region around H-point indicates the strongest EPC contributions. The yellow/orange regions around Γ- and A-point indicate the 2nd strongest EPC contributions. Figs. S1(b-d) show the evolutions of the superconducting gap distributions along with increasing temperature from 5 K, 15 K, to 25 K near the transition temperature, respectively. Figs. S1(b,c) ($T = 5\ K$, $T = 15\ K$) show that the large superconducting gap of $\Delta_2 = 5.06$ meV (red region) distributes around $k = 0.4\ \overrightarrow{KH}$. Small superconductivity gap region $\Delta_1 = 4.01$ meV can be found near $k = 0.25\ \overrightarrow{\Gamma A}$ to $k = 0.65\ \overrightarrow{\Gamma A}$ yellow/orange region. They agree well with the EPC distributions in Fig. S1(a). At $T = 25\ K$ near the transition temperature, Fig. S1(d) shows that Δ_2 superconductivity gap decreases to 2.2 meV and Δ_1 superconductivity gap decreases to 1.2 meV. These results are consistent with the superconductivity gap distribution in Fig. 4(b) and quasiparticle density of sates results in Fig. 4(c-d).

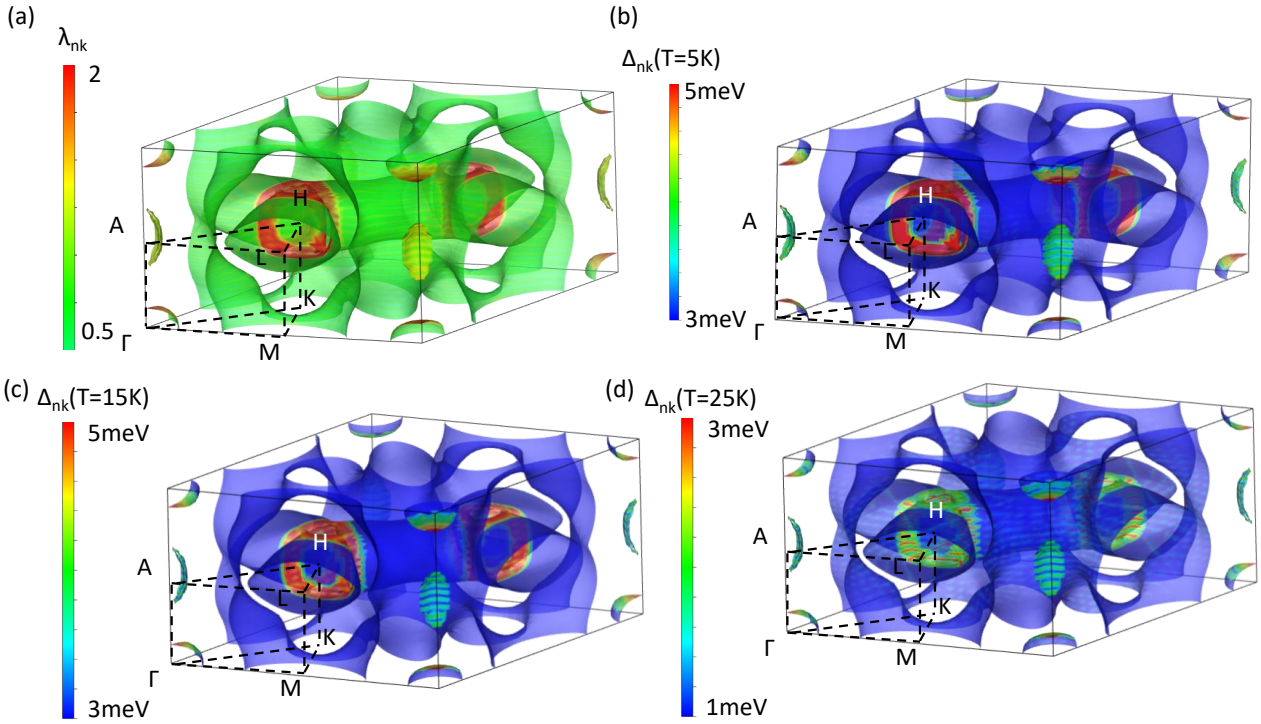

Fig. S1: (a) Momentum-resolved EPC at FS of LaB_2 (The same as Fig. 3d in the main text). (b)-(d): Momentum-resolved superconducting gap at T=5K, T=15, T=25K, respectively.

II. TOPOLOGICAL RESULT

To study spin-orbital coupling (SOC) induced topological property, Fig. S2 shows SOC induced continuous gap in the yellow region. The calculated Wilson loop between this continues gap are shown in Fig. 5 of the main text. The resultant close Wilson loop at k_x and k_y time-reversal plane and open Wilson loop at k_z time-reversal plane lead to the topological number $\mathbb{Z}_2 = (0, 001)$, indicating the system is topologically non-trivial. At $(1\bar{1}0)$ and (010) surfaces, the electronic spectrum show topological non-trivial surface states crossing with each other within the bulk state energy gap as shown in Fig. S3 and Fig. S4, respectively. Whereas at the (001) surface, no surface state can be found within the bulk continue gap energy region at top surface and bottom surfaces as shown in Fig. S5.

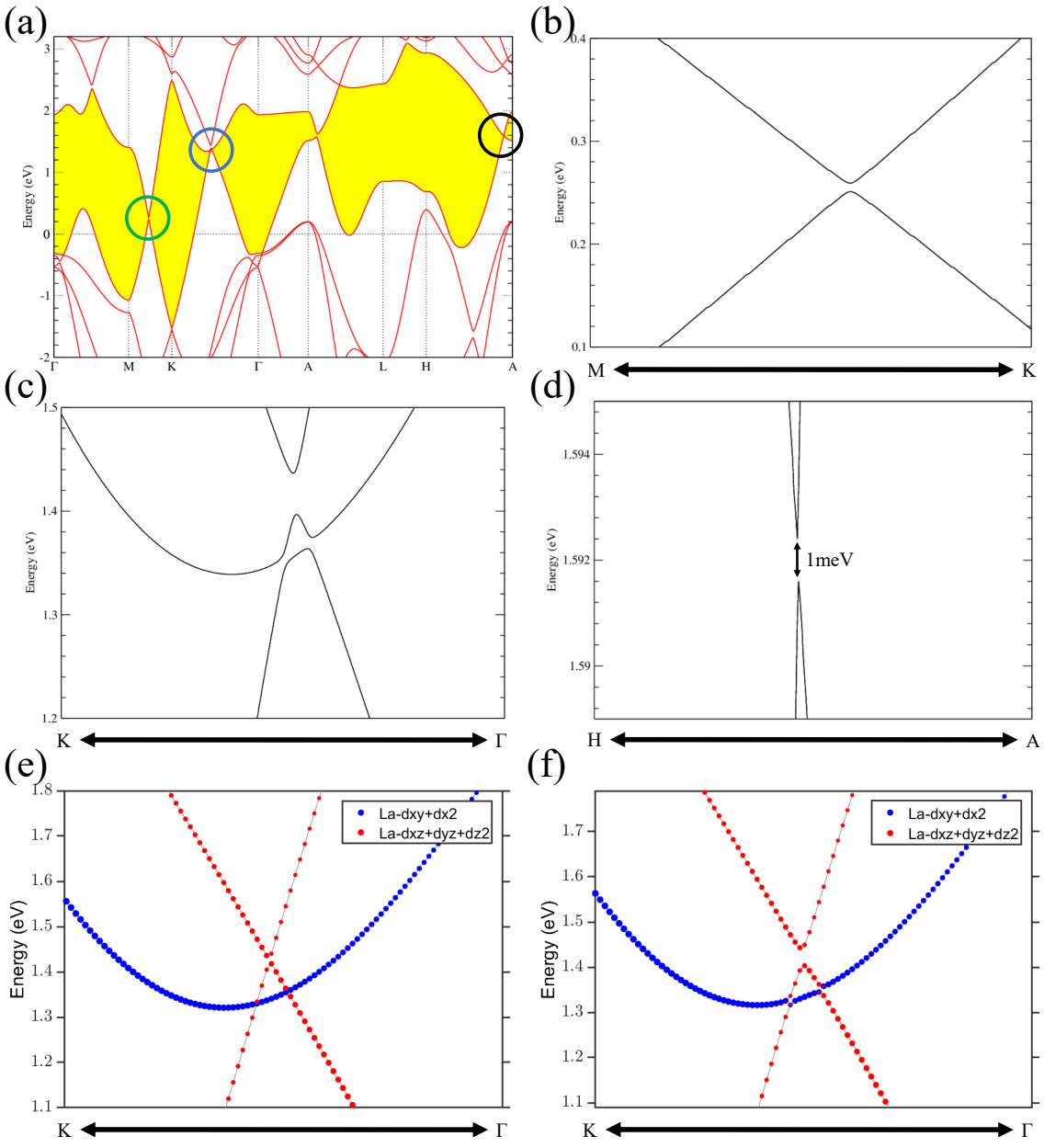

Fig. S2: (a) Spin-orbit coupling band structure. Yellow region highlights SOC induced continuous gap. (b)-(d) Zoom in (a) at the green, blue, and black circles, respectively. (e)-(f) The electronic band structure of LaB_2 without and with SOC, respectively, projected onto the La-$(d_{xy} + d_{x^2+y^2})$ and La-$(d_{xz} + d_{yz} + d_{z^2})$ orbitals along k-path $K\Gamma$ around the blue circle in (a). Topological band inversion can be found around the continuous band gap due to SOC (f).

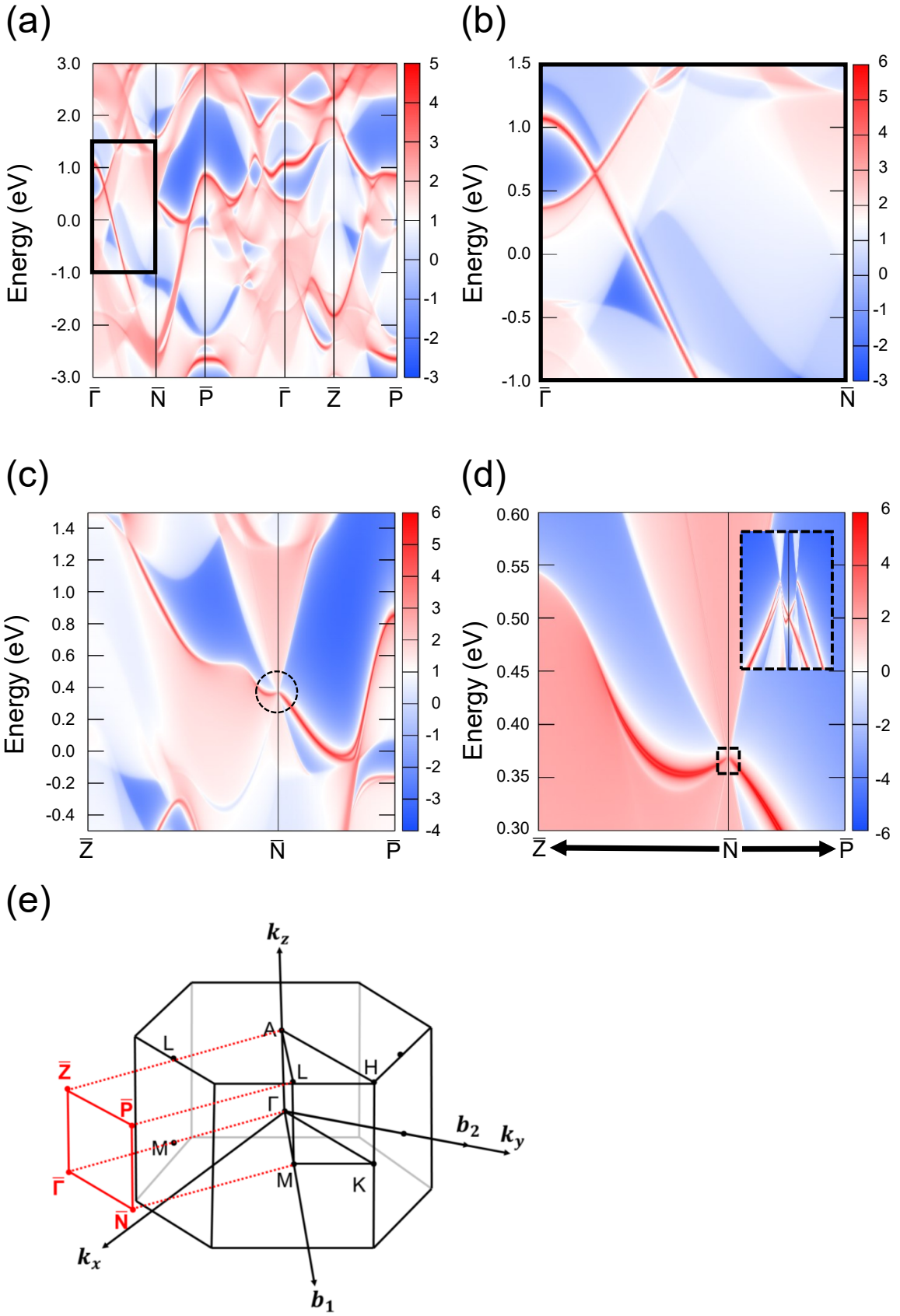

Fig. S3: (a) The surface spectrum of LaB_2 at $(1\bar{1}0)$ plane. The black solid square frame shows the topological surface state (red crossing band). The band structure of the top and bottom surfaces are the same and only one of them is shown here. (b) Zoom in black solid square frame in (a). (c) The surface spectrum of LaB_2 in high-symmetry points $\bar{Z}$-$\bar{N}$-$\bar{P}$. The black dashed circle shows another topological surface state. (d) Zoom in black dashed circle in (c). (e) The projected surface Brillouin zone of $(1\bar{1}0)$ planes on Hexagonal Brillouin zone. High symmetry points and frame lines represent bulk BZ and $(1\bar{1}0)$ surface BZ in black and red, respectively. Color bars are represented on a log scale with red, white and blue color for surface state, bulk state and no state.

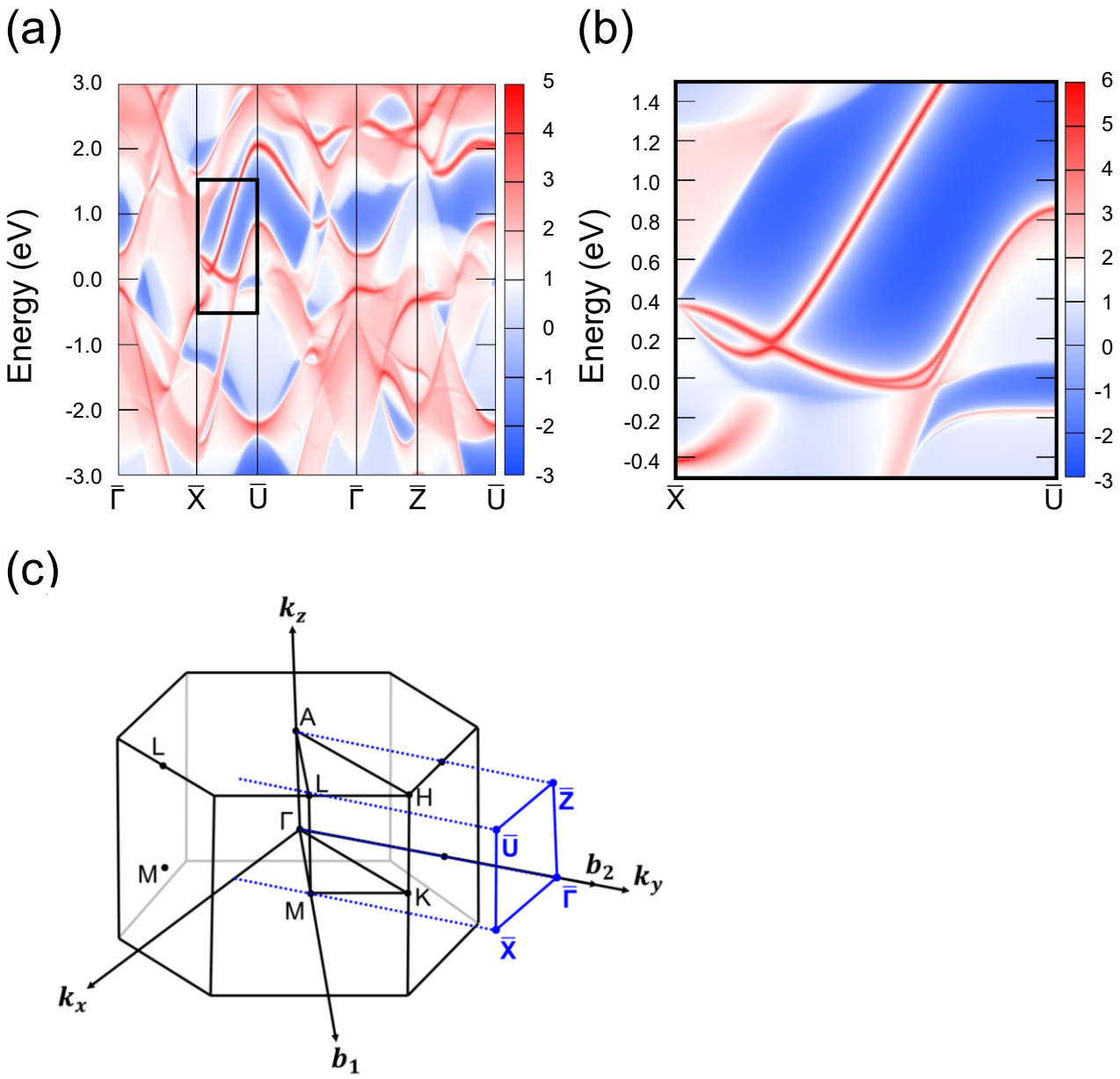

Fig. S4: (a) The surface spectrum of LaB_2 at (010) plane. The black solid square frame shows the topological surface state. (b) Zoom in the black solid square frame in (a). (c)The projected surface Brillouin zone of (010) planes on Hexagonal Brillouin zone. The atoms on the top and bottom surfaces are lanthanum and boron, respectively, and thus have different surface states. Topological surface states can be seen on the top surface as shown in (a), (b). High symmetry points and frame lines represent bulk BZ and (010) surface BZ in black and blue, respectively. The specifications of the color bars are the same as in Fig. S3.

* These authors contributed equally to this work.
† jeng@phys.nthu.edu.tw

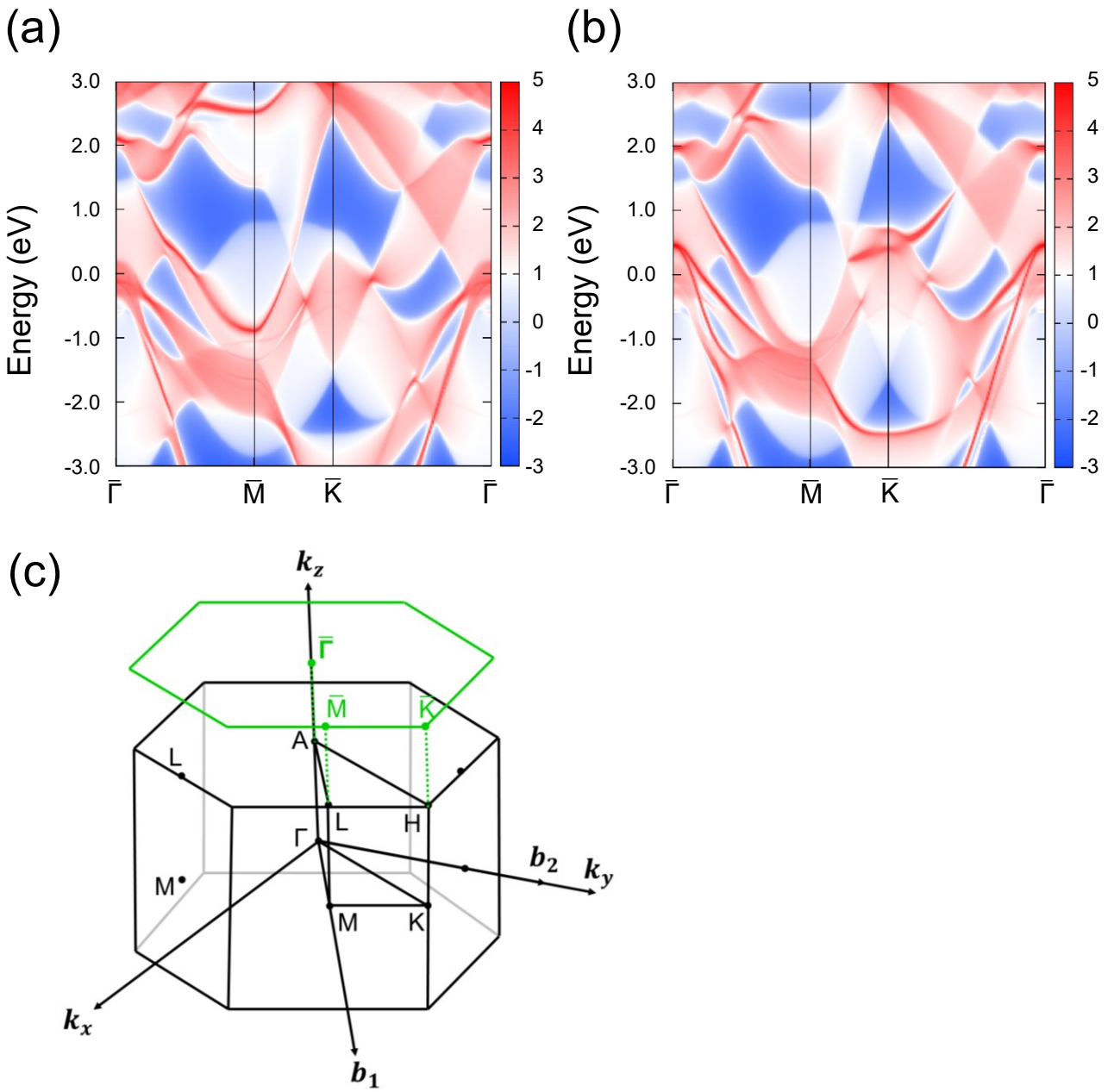

Fig. S5: (a)-(b) The top and bottom surface spectra of LaB_2 at (001) plane. No topological surface states can be found on (001) planes. (c)The projected surface Brillouin zone of (001) planes on Hexagonal Brillouin zone. High symmetry points and frame lines represent bulk BZ and (001) surface BZ in black and green, respectively. The specifications of the color bars are the same as in Fig. S3.